Chemical Engineering Journal 391 (2020) 123510

Contents lists available at ScienceDirect

Chemical Engineering Journal

journal homepage: www.elsevier.com/locate/cej

High-performance quasi-solid-state flexible sodium metal battery: Substrate-free FeS_2–C composite fibers cathode and polyimide film-stuck sodium metal anode

Jagdeep Mohanta[a], Hye-Jung Kim[b], Sang Mun Jeong[a,*], Jung Sang Cho[c], Hyo-Jun Ahn[d], Jou-Hyeon Ahn[d,*], Jae-Kwang Kim[b,*]

[a] Department of Chemical Engineering, Chungbuk National University, 1 Chungdae-ro, Seowon-gu, Cheongju, Chungbuk 28644, Republic of Korea
[b] Department of Solar & Energy Engineering, Cheongju University, Cheongju, Chungbuk 28503, Republic of Korea
[c] Department of Engineering Chemistry, Chungbuk National University, Chungbuk 361-763, Republic of Korea
[d] Department of Materials Engineering and Convergence Technology and RIGET, Gyeongsang National University, 501 Jinju-daero, Jinju 52828, Republic of Korea

HIGHLIGHTS

- A substrate-free carbon-coated FeS_2 fiber-based cathode is prepared by electrospinning.
- Sodium metal on the polyimide film provides a high flexible sodium metal battery.
- Discharge capacity of 808.26 mAh g^{-1} is obtained with the flexible sodium metal battery.
- The flexible sodium metal battery allows high reversibility and electrochemical stability.

GRAPHICAL ABSTRACT

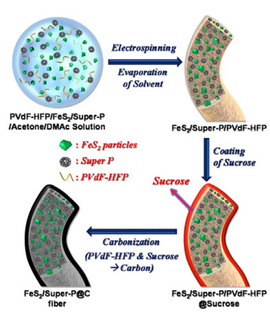

ARTICLE INFO

Keywords:
FeS_2 fiber
Substrate-free electrode
Electrospinning
Hybrid solid electrolyte
Solid-state flexible sodium metal battery

ABSTRACT

A substrate-free carbon-coated FeS_2-fiber-based cathode for quasi-solid-state rechargeable flexible sodium metal batteries is reported for the first time. A facile electrospinning technique followed by carbonization is employed for the synthesis of a novel cathode for a flexible sodium metal batteries. For fabrication of the solid-state flexible battery, a $Na_3Zr_2Si_2PO_{12}$-based hybrid solid electrolyte is utilized as the separator and electrolyte. A discharge capacity of about 808.26 mAh g^{-1} is obtained in the first charge–discharge cycle, which is greater than that of any previously reported Na/FeS_2-based battery. The carbon coating on the FeS_2 fiber allows the flexible battery to have an enhanced discharge capacity of 633.43 mAh g^{-1}, even after undergoing five charge–discharge cycles at a 0.1 C rate. At a 2 C rate, a high specific capacity of 393.5 mAh g^{-1} is maintained, and the value increases on the return from 2 C to 0.1 C until it reaches a value similar to the initial 0.1 C rate. A superior rate capability with enhanced electrochemical stability of the quasi-solid-state sodium metal battery is also demonstrated due to the substrate-free flexible carbon-coated FeS_2-fiber-based cathode. Owing to its high flexibility and electrochemical properties, the flexible solid-state sodium metal battery has considerable potential for high-performance sodium batteries.

* Corresponding authors.
E-mail addresses: smjeong@chungbuk.ac.kr (S.M. Jeong), jhahn@gnu.ac.kr (J.-H. Ahn), jaekwang@cju.ac.kr (J.-K. Kim).

https://doi.org/10.1016/j.cej.2019.123510
Received 28 July 2019; Received in revised form 5 November 2019; Accepted 14 November 2019
Available online 16 November 2019
1385-8947/

1. Introduction

The perpetual upsurge in population and industry over time creates a situation where it becomes essential to produce and store enormous amount of energy, both now and for future generations. Therefore, the development of improved energy storage systems that can safely hoard more energy for longer periods of time is required. Lithium ion batteries (LIBs) are a well-commercialized energy storage system, but when it comes to large-scale energy storage, LIBs have many drawbacks, such as the scarcity of lithium in the earth's crust and the extreme hygroscopic nature of lithium. In contrast, the vast profusion of sodium in nature, excellent safety, and a mechanism for hoarding energy similar to that of the LIB makes the sodium metal battery (SMB) an efficient candidate for an energy storage system [1–4]. Like the cathode materials in LIBs, the cathode materials in rechargeable SMBs get significant attention because many electrochemical parameters, such as cycle life and specific capacity, depend on the nature of the cathode materials employed [5–8]. Transition metal sulfides such as CoS_2, CuS_2, and NiS_2 have been particularly exploited as cathode materials owing to the involvement of a conversion reaction rather than an intercalation reaction, which induces greater capacity to the battery. Among them, iron disulfide (FeS_2) has been very intriguing because of significant advantages such as economical value, environmental friendliness, and a high abundance in nature [9,10]. Despite such features, the pristine FeS_2 cathode faces some limitations; one of the prime disadvantages is polysulfide dissolution during charging and discharging [11]. Many studies have recently tried different approaches to address this issue [12–15]. Of these various ways, applying a uniform carbon coating is the most effective solution for preventing polysulfide dissolution. In addition to solving the above-mentioned problem, carbon coating has been proven to be beneficial for cathode materials as it contributes to better electronic conductivity and superior electrochemical performance in the battery [16,17]. Recently, Haridas et al. utilized a novel technique to prepare an FeS_2/C nanofiber web and used it as a cathode material in rechargeable LIBs. This battery displays an enhanced discharge capacity of 545 mAh g^{-1} even after 500 charge–discharge cycles at a charging rate of 1 C. In addition, this material demonstrates high retention capacity as well as better cycle stability [18]. Although the FeS_2 cathode is much improved in lithium ion battery systems, it still shows poor electrochemical performance in sodium ion batteries. Therefore, a novel strategy is required to improve the properties of FeS_2-based sodium ion batteries.

Conventionally, many additional substances such as binders and current collectors are incorporated during preparation of the SMB cathode, which makes the cell more bulky and rigid and thus affects the efficiency of the battery. Hence, it is essential to develop flexible and free-standing cathodes that can give improved performance and allow for more flexible sodium battery designs [19–22]. Yuan et al. utilized a flexible $Na_4Mn_9O_{18}$/reduced graphene oxide (NMO-RGO) hybrid film as the cathode for a SMB, which helps make the electrode cost effective while delivering excellent electrochemical performance with 83 mAh g^{-1} [23]. Improved reversibility in specific capacity, better rate capability, and greater cycle stability have been reported by using a flexible metal–organic framework consisting of Prussian blue analogue $Fe(CN)_6$/carbon cloth composites [24]. In another study, Song et al. demonstrated $Na_2FeP_2O_7$ nanoparticles entrenched in porous carbon cloth as a freestanding cathode for a SMB and reported excellent capacity retention with 82 mAh g^{-1} [25]. All the recent studies on flexible cathodes for SMBs described above display enhanced properties but they all showed low discharge capacity and involved the use of substrates such as carbon paper or zinc sheets for providing the flexibility to the cathodes as well as the enhanced mechanical and conductivity properties. Therefore, there are still issues associated with the low capacity, the use of substrates in the cathodes and liquid electrolytes of SMBs such as cost, excess weight, and extra rigidity that affect the properties of the flexible cathodes [19].

Therefore, in the present work, for the first time we report a substrate-free flexible carbon-coated FeS_2 fibers (FeS_2/C) based cathode for rechargeable quasi-solid-state flexible SMBs, prepared by employing a facile electrospinning technique using commercially available iron sulfide. A uniform carbon coating is applied over the FeS_2 cathode to achieve better electrochemical properties by diminishing the polysulfide dissolution; it also plays a significant role in providing flexibility with a hybrid solid electrolyte to the prepared SMB. This cathode material is then employed to make a flexible pouch cell SMB with a sodium metal anode, which displays superior electrochemical features such as a large discharge capacity of 808.26 mAh g^{-1} for the first charge–-discharge cycle with enhanced coulombic efficiency retention of 88% even after the completion of five cycles. High electrochemical stability and rate capability is also exhibited. The unique structure of the carbon-coated fibrous FeS_2 electrode not only prevents dissolution of the polysulfide, but also improves the flexibility of the solid-state sodium metal battery as well as the electrochemical reaction by increasing the migration rate of electrons and ions.

2. Experimental

For fabrication of the FeS_2/C fibers, FeS_2 (10 g), super-p carbon black (2 g), and poly(vinylidene fluoride-*co*-hexafluoropropylene) (PVdF-HFP, 6 g) was incorporated into 7:3 acetone:dimethylacetamide (DMAc). The components were homogeneously mixed by stirring for approximately 12 h. Electrospinning was then performed on the prepared solution using a 10 mL syringe attached to a syringe pump (Model 210, KD Scientific) at a flow rate of 0.1 mL min^{-1}. The voltage applied and distance between the metallic needle and rotating collector was 12 kV and 15 cm, respectively. This resulted in the formation of fibers composed of FeS_2 and PVdF-HFP. To prevent the fibers from undergoing aggregation during carbonization of the sample, the fibers were first immersed in a sucrose solution (13 wt% of sucrose in ethanol) and air dried. Carbonization of the fibers was carried out by calcination at 500 °C for 5 h in an argon atmosphere at a rate of 10 °C min^{-1}. This resulted in the creation of FeS_2/C fibers. Scheme 1 depicts the synthesis procedure.

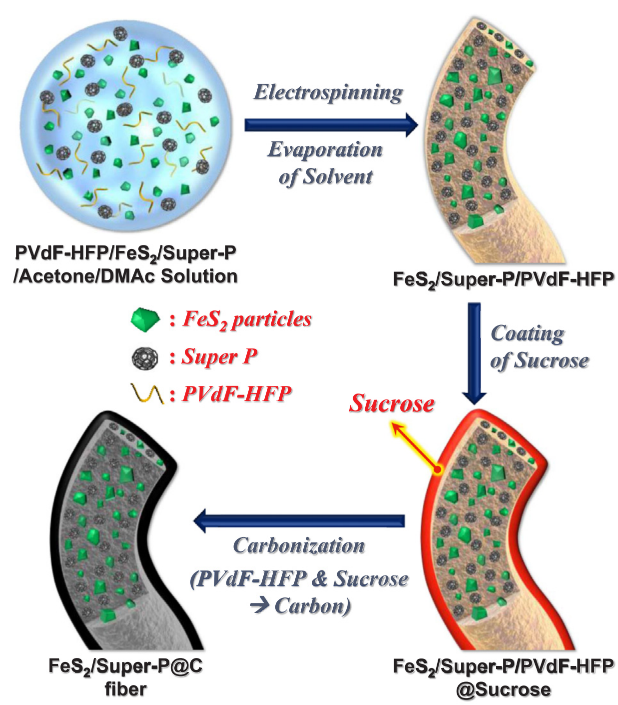

Scheme 1. FeS_2/C fiber preparation.

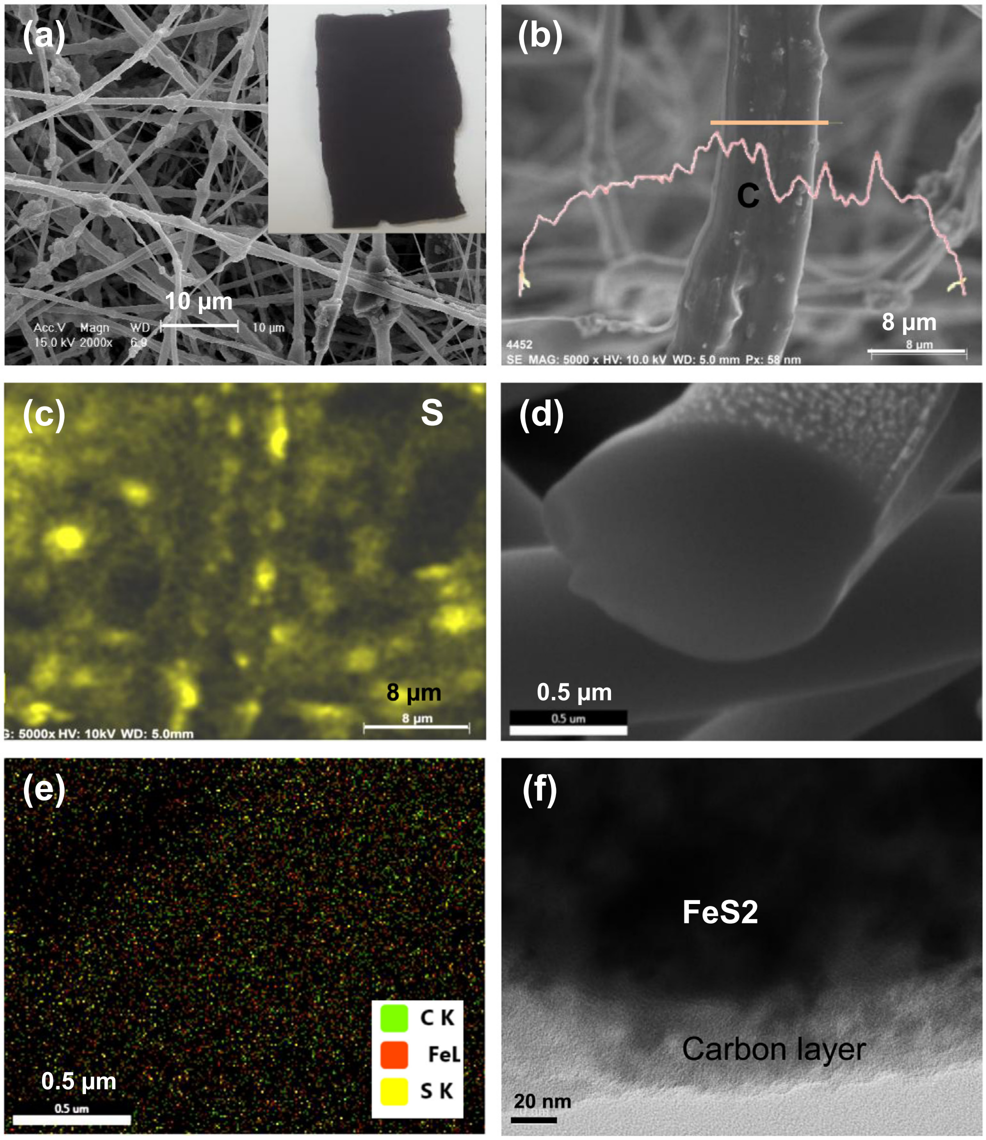

Fig. 1. (a) FE-SEM of FeS_2/C fiber (inserted figure: Photo image of FeS_2/C fiber electrode). (b) EDS line spectra of carbon, (c) elemental mapping of sulfur in FeS_2/C fiber. (d) Focused-ion beam image, (e) EDAX, and (f) TEM image of FeS_2/C fiber.

X-ray diffraction (XRD) of the prepared substrate-free flexible FeS_2/C fibers was carried out for structural analysis by employing a D2 Phaser Bruker AXS with CuK_α radiation. A Philips XL305 FEG field emission scanning electron microscope (FE-SEM) was utilized for the morphological study of the FeS_2/C fibers. To determine the amount of carbon coated on the FeS_2, transmission electron microscopy (TEM) was performed using a TF30ST-300 kV microscope (TECNAI). Elemental analysis was carried out with a Thermo Fisher Scientific Flash 2000 Series instrument. A VG Scientific ESCALAB 250 was employed to measure the ex-situ X-ray photoelectron spectra (XPS) of the fresh, charged, and discharged FeS_2/C electrode. For conductivity measurements, a four-point probe analyzer (ARMS-300C, Dasol Eng) was used.

For preparation of the cathode, the FeS_2/C fibers film was dried in a vacuum oven for 12 h at 80 °C. The mass load on the circular electrodes was 3.6 ± 0.1 mg cm^{-2}. Using sodium foil as the anode, pouch cells were prepared inside an argon-filled glove box where H_2O and O_2 levels were maintained below 10 ppm. Hybrid solid electrolyte ($Na_3Zr_2Si_2PO_{12}$ + PVdF-HFP + $NaCF_3SO_3$/TEGDME composite) was employed as the electrolyte for carrying out the electrochemical investigation of FeS_2/C as an electrode [20]. Sodium-conducting NASICON-type $Na_3Zr_2Si_2PO_{12}$ solid electrolyte was prepared by a solid-state reaction method [26]. The $Na_3Zr_2Si_2PO_{12}$ ceramic powder was mixed with PVdF-HFP solution to prepare a hybrid film and the hybrid solid electrolyte was prepared by soaking the 1 M $NaCF_3SO_3$/TEGDME (15 wt%) into the hybrid film (85 wt%). A WBCS 3000 electrochemical workstation from WonA Tech. Co. was employed to perform the electrochemical tests at various C-rates. Cyclic voltammetry was performed at a scan rate of 0.1 mV s^{-1}. An IM6 impedance analyzer (Zahner Elektrik) was used for impedance spectroscopy.

3. Results and discussion

A simple electrospinning procedure was employed to prepare the FeS_2/C fibers from a low-cost iron sulfide (Scheme 1). The natural FeS_2 powder was pulverized by ball milling before preparation of the mixture for electrospinning. Dipping the fibers in a sucrose solution plays a crucial role in maintaining the fibrous structure. Both carbonization and disintegration of PVdF-HFP occur when the sucrose-containing fibers are subjected to heat treatment for 5 h at 500 °C.

The XRD spectra of the FeS_2 powder and synthesized FeS_2/C fiber are depicted in Fig. S1a. A cubic phase for both the FeS_2 powder and

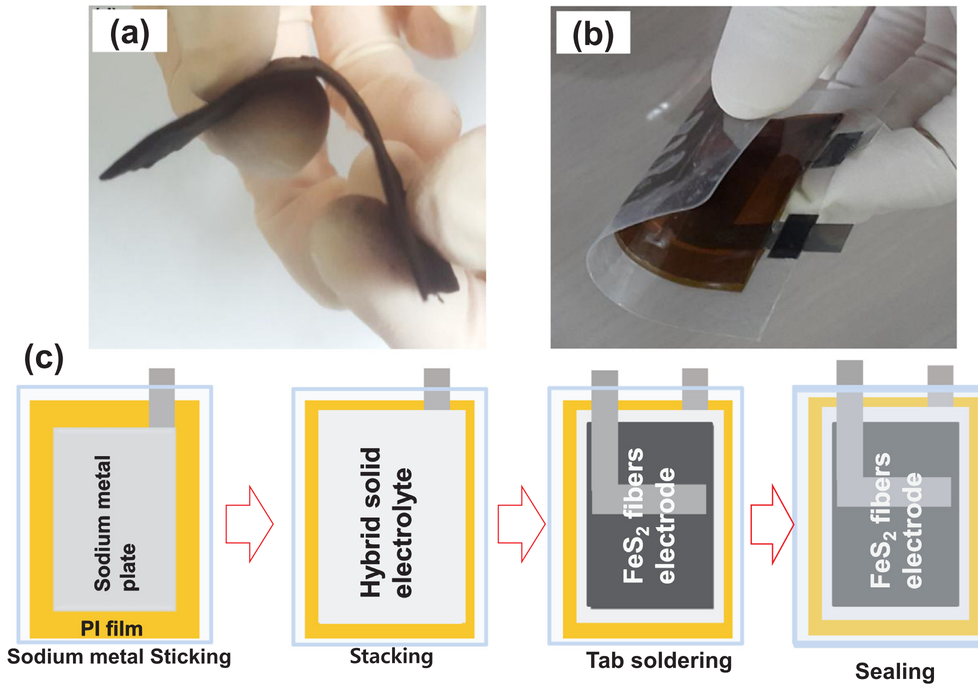

Fig. 2. (a) Flexibility of FeS_2/C fiber electrodes and (b) pouch cell containing FeS_2/C fiber as the cathode and hybrid solid electrolyte as the electrolyte. (c) Process of preparation for solid-state flexible FeS_2 sodium metal battery.

FeS_2/C fiber is indicated from the diffraction peaks, which are in good accordance with JCPDS no. 42-1340 [27]. High crystallinity of the synthesized material is demonstrated through the sharp and robust diffraction peaks in the XRD spectrum. An additional diffraction peak at 38.7 is seen in the FeS_2/C fiber, which may be due to the aluminum substrate used during electrospinning. Because the XRD spectra of FeS_2 and FeS_2/C are similar, the crystal structure of FeS_2/C can be assumed to be the same as FeS_2. Fig. S1b shows the crystal structure of FeS_2. Each sulfur atom is coordinated with three iron atoms and with its dimer pair, while six sulfur atoms are bonded to each iron atom in a tempered octahedron. The crystal structure is somewhat similar to that of sodium chloride, with the disulfide ions occupying the midpoints of the body center and edges of the cubic structure, whereas the fcc sublattice sites are dominated by ferrous ions.

The morphology of the FeS_2/C fiber was determined by FE-SEM (Fig. 1a). Well-formed FeS_2/C fibers can be seen. Small humps present between the fibers may be due to aggregation of the FeS_2 particles employed in the synthesis. The aggregation of the particles at the intersections of the fibers primarily occurs as a result of the attraction of the high-density portions during the electrospinning. The average fiber diameter, as calculated from the FE-SEM image using image software, was found to be 1.13 µm. The inserted figure in Fig. 1a shows a portion of the synthesized FeS_2/C fiber electrode. The electrode has a fiber network which increases the effective area between the electrode and hybrid solid electrolyte during cell assembly pressing. The fiber network is highly efficient for fast ion transfer and has robust flexibility. The presence of the carbon coating on the FeS_2 fibers is evident from the EDS line spectra of carbon taken across a FeS_2/C fiber (Fig. 1b). The highest percentage of carbon is across the FeS_2/C fiber, and the proportion of carbon decreases at the edge because of the round form. Elemental mapping of sulfur (Fig. 1c) confirms that it is uniformly distributed in the FeS_2/C fibers. Moreover, in comparing Fig. 1c to Fig. 1a, it can be seen that there is high concentration of sulfur atoms where the particles are aggregated. Fig. 1d shows focused-ion beam (FIB) images of a FeS_2/C fiber. The FeS_2/C fiber is cut at a point 1 µm from the top in order to observe the inside of the fiber. It can be seen that there is no empty space in the FeS_2/C fiber. Fig. 1e shows the results of EDX mapping of the cut cross-section shown in Fig. 1d. The green, red, and yellow points represent the carbon (C), iron (Fe), and sulfur (S) signal counts, respectively, in the entire area. The consistent signal counts indicate that the FeS_2 and C are uniformly distributed. Additionally, TEM of a FeS_2/C fiber was carried out and a fine carbon layer of around 45 nm can be seen around the substrate-free FeS_2 fiber (Fig. 1f). The uniformly coated carbon on the FeS_2 might enhance the mobility of the electrons in the SMB during the electrochemical redox reaction of FeS_2 by allowing better ion conduction between the electrode and the electrolyte within the SMB. The stability of FeS_2 fibers after carbon encapsulation was further ascertained through the XPS spectra of Fe before and after carbonization of FeS_2 fibers as displayed in Fig. S2. As it can be seen there is hardly any deviation in the Fe spectra in the XPS plot of FeS_2 fibers before and after carbonization.

The flexibility of the FeS_2/C fiber electrode is displayed in Fig. 2a. The fiber network structure provides high flexibility to the FeS_2-based electrode. To prepare the flexible sodium metal electrode, novel electrode constitution was designed that the sodium metal plate was stuck on the polyimide film (Fig. 2c). Furthermore, when the FeS_2/C fiber electrode without metal substrate was incorporated into a pouch cell battery with sodium metal as the anode and $Na_3Zr_2Si_2PO_{12}$-based hybrid solid electrolyte as the electrolyte, it can be seen that the pouch cell is as highly flexible as the FeS_2/C fiber cathode (Fig. 2b). The absence of the metal substrate may increase the energy density of flexible batteries and the hybrid solid electrolyte may improve the stability of the sodium metal electrode [28]. The hybrid solid electrolyte displays high flexibility in the solid phase and a high ionic conductivity of 1.06×10^{-3} S cm^{-1} at 30 °C (Fig. S3). The flexibility of the cathode and ultimately of the battery is a result of the even coating of carbon on the surface of the fiber network -type FeS_2, polyimide film, and film-type hybrid solid electrolyte.

Charge–discharge studies were carried out to scrutinize the electrochemical properties of the FeS_2/C fiber cathode. The charge–-discharge curves for three different cycles of a pouch cell containing a FeS_2/C fiber cathode, hybrid solid electrolyte, and sodium metal anode with a C-rate of 0.1 C is shown in Fig. 3a. Owing to the presence of the FeS_2/C fiber cathode, a large discharge capacity of 808.26 mAh g^{-1}

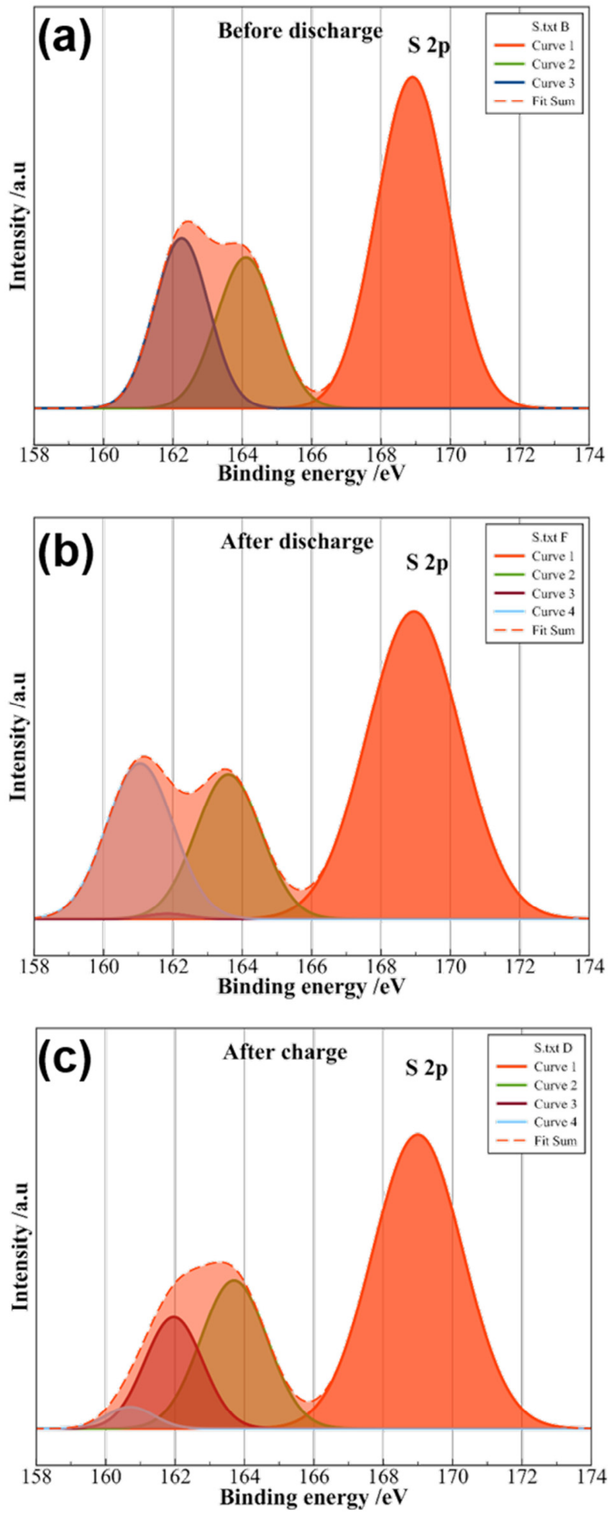

Fig. 3. Ex-situ XPS analysis of FeS_2/C fiber cathode displaying the variations in S 2p spectra (a) before discharge, (b) after discharge, and (c) after charge.

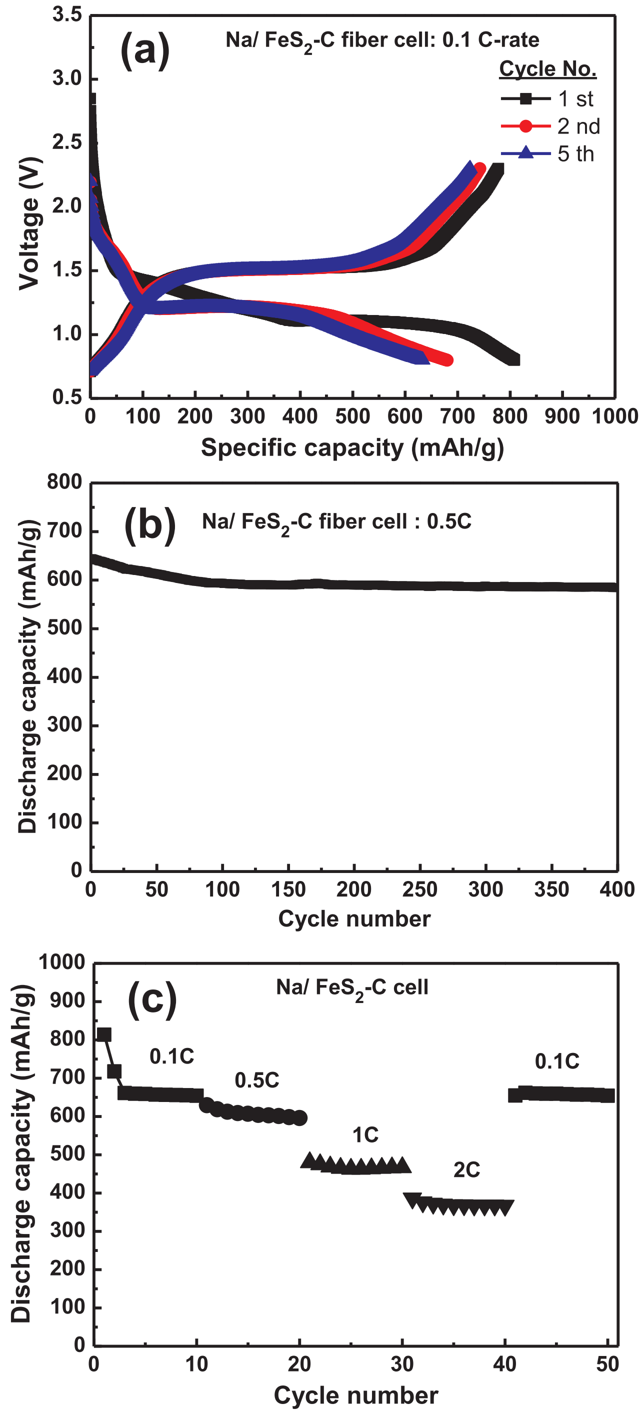

Fig. 4. (a) Charge–discharge plot of Na/HSE/FeS_2/C fiber cell at 0.1 C-rate. (b) Cycle life of Na/HSE/FeS_2/C fiber cell at 0.5 C-rate. (c) Rate capability plot of Na/HSE/FeS_2/C fiber solid-state cell.

was observed for the first cycle, which is higher than that of previously reported SMBs that contain FeS_2 cathodes [9,29]. There is a minimum reduction in discharge capacity of ~22% after the fifth cycle. The capacity fading is much less owing to the dense coating of carbon on the FeS_2 fiber. The first charge–discharge cycle displays a coulombic efficiency as high as 97%, which obviously decreases in subsequent cycles, but 88% of the coulombic efficiency is still sustained after the fifth cycle. Therefore, the carbon coating over the FeS_2 fiber leads to enhanced coulombic efficiency with a large discharge capacity, even after completion of five charge–discharge cycles. The XPS of the FeS_2/C fibers during the charge–discharge cycle indicate that in the initial state, the 2p3/2 peak for Fe^{2+} was obtained at around 711 eV, which then shifts to around 710 eV during the discharge state, indicating a change in the oxidation state of iron from Fe^{2+} to Fe^0 upon discharging (Fig. S4) [9]. Fig. 3b displays the cycling performance of the FeS_2/C fiber cathode at 0.5 C, and it is observed that even after undergoing 400 charge–discharge cycles, the cell upholds a high discharge capacity of around 90% of the initial discharge capacity of 644.37 mAh g^{-1}. For comparison, the cycling performance of bare FeS_2 was studied (Fig. S5),

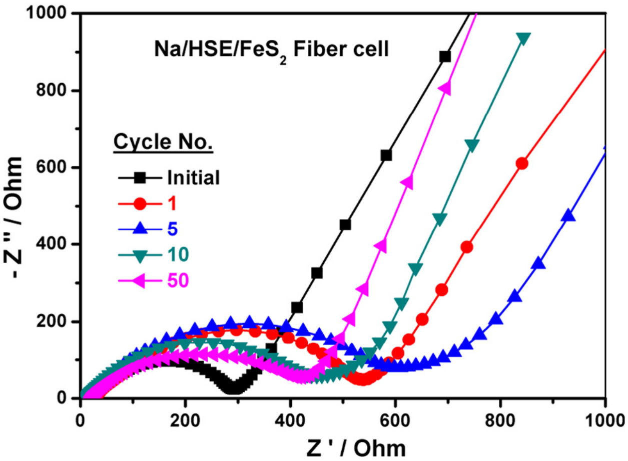

Fig. 5. Nyquist impedance plot of flexible substrate-free carbon-coated FeS_2/C fiber solid-state cells.

and it was observed that the discharge capacity with a bare FeS_2 cathode was initially below 600 mAh g^{-1}, which then significantly decreased with increasing cycle number. Hence, the FeS_2/C fiber cathode also leads to improved cyclability of the solid-state SMB. The stable cycle performance of the quasi-solid-state FeS_2/C cell is ascribed to the carbon coating and hybrid solid electrolyte preventing the dissolution of the polysulfide produced during the electrochemical reaction. Enhanced cycle life is further depicted by the FE-SEM image of the FeS_2/C fiber cathode (Fig. S6), where we observe that the fibrous structure of the FeS_2/C fiber cathode remains robust even after undergoing 300 charge–discharge cycles, and the fibers only appear to grow in size. The carbon coating over the FeS_2 plays a vital role in maintaining the fibrous structures of the FeS_2/C fiber cathode after so many charge/discharge cycles. To see the impact of bending of the cell on discharge capacity. The discharge capacity of the cell at different deformation i.e. flatness, bending and again re-flatness has been depicted in Fig. S7. As it is been clearly observed very minute reduction in the value of discharge capacity on going from flat position to bending position, indicating excellent electrochemical properties of the cell even at bending of it. Furthermore, from the rate capability of the cell (Fig. 3c), a decrease in discharge capacity is observed as the C-rate is increased from 0.1 C to 2 C. However, excellent reversibility is displayed by the cell, as the discharge capacity is almost the same as the initial 0.1 C rate when the C-rate returns from 2 C to 0.1 C [30]. Hence, as expected, it is found that the electrochemical properties are enhanced due to the presence of the carbon over the FeS_2. Fig. S8 displays the cyclic voltammetry of the first three cycles with a scan voltage of 0.1 mV s^{-1}. It can be seen there is hardly any difference in the three cycles. All three cycles show one cathodic and anodic peak at 1.12 V and 1.5 V, respectively. This indicates the occurrence of a single-step reduction and single-step oxidation of FeS_2 by two sodium ions. Hence, the charge and discharge reaction in the present SMB could be represented by the following equations:

$$2Na^{+} + 2e^{-} + FeS_2 \rightarrow Na_2FeS_2 \quad (1)$$

$$2Na^{+} + 2e^{-} + Na_2FeS_2 \rightarrow Na_2S + Fe \quad (2)$$

Moreover, the presence of only one redox couple indicates good electrochemical stability of the cells [9,31,32].

To ascertain the mechanism of sodiation and desodiation, the ex-situ S 2p XPS spectra of the FeS_2/C fiber electrode were taken during charging and discharging (Fig. 4). Two major peaks at 164.1 and 162.2 were observed before discharge, which can be ascribed to S $2p_{1/2}$ and S $2p_{3/2}$ of FeS_2 [33]. Oxidized sulfate species from the electrolyte results in generation of XPS peaks at 165–170 eV. In the case of the FeS_2/C fiber electrode, such a peak is seen around 169 eV, is attributed to oxidized SO_x, and remains during charging and discharging [18]. A new peak occurred around 160.9 eV, along with slight shifts of the characteristic peaks (i.e., 164.1 and 162.0 eV) on discharging due to the formation of Na_2S. After charging, the formed Na_2S was still present with an increased S $2p_{3/2}$ peak of FeS_2 (162.0 eV) because of the irreversible reaction at the first cycling. The Na 1s XPS spectra (Fig. S9) further revealed that, before discharge, there is no peak, but after discharge, a peak is generated around 1072 eV, which is ascribed to the Na ion. After charging, the peak again vanishes, which indicates good Na hoarding competence of the FeS_2/C fiber cathode [34,35].

The Nyquist impedance plot (Fig. 5) initially demonstrates low bulk resistance and high ionic conductivity of the cell due to the existence of the bulky triflate ($CF_3SO_3^{-}$) anion absorbed into the hybrid solid electrolyte. However, during the first cycle, a solid electrolyte interface (SEI) layer was created on the surface of the Na anode, which leads to significant enhancement in bulk resistance. Similarly, there is slight increase in bulk resistance in the fifth cycle. Finally, after the fifth cycle the SEI layer becomes stable and a reduction in bulk resistance in further cycles is observed, i.e., the tenth and fiftieth cycles. To prepare the hybrid solid electrolyte, the incorporation of 15 wt% $NaCF_3SO_3$/TEGDME not only reduces the boundary resistance in the electrolyte, but also significantly reduces the interfacial resistance with the electrodes [20,36,37]. The reduced resistance improves ion mobility, allowing excellent electrochemical properties in quasi-solid-state flexible SMBs. Furthermore, the impedance plot of the cell at different bending strain was also plotted (Fig. S10). The plot at flat mode and bending mode are almost similar with a minor deviation (~15 Ohm) displaying negligible impact of bending on performance of cell.

4. Conclusions

This work demonstrates a novel strategy to enhance the electrochemical properties of quasi-solid-state FeS_2 flexible sodium metal batteries (SMBs) by using a substrate-free carbon-coated FeS_2 fiber-based cathode and NASICON-type hybrid solid electrolyte. Crystallographic structure determination by XRD indicates that FeS_2/C has a cubic structure. FE-SEM and TEM images indicate the formation of FeS_2 fibers and the presence of a carbon coating, respectively. Owing to the successful even coating of carbon upon FeS_2, better electronic conductivity and hence excellent electrochemical features have been displayed by a solid-state flexible SMB pouch cell incorporating FeS_2/C as the cathode, $Na_3Zr_2Si_2PO_{12}$-based hybrid solid electrolyte as the electrolyte, and sodium metal as the anode. Polysulfide dissolution, which is a major hindrance in using FeS_2 as a cathode material, has been circumvented by the use of a carbon coating over FeS_2 and a hybrid solid electrolyte. The polyimide substrate on the sodium metal electrode and the carbon coating are also responsible for providing flexibility to the SMB and better ion conduction between the electrode and the electrolyte. Charge–discharge analysis depicts an enhanced discharge capacity of 808.26 mAh g^{-1} in the first charge–discharge cycle, with high coulombic efficiency retention of 88% even after five charge–discharge cycles. Rate capability and cyclic voltammetry tests of the cell indicate good reversibility and enhanced electrochemical stability, respectively. Moreover, the fibrous structure of FeS_2/C remains intact even after 300 charge–discharge cycles. Hence, the present work represents a design of flexible sodium metal batteries using sodium metal anode and a simple technique to prepare FeS_2/C fibers, which are employed for the first time as an effective cathode material for a rechargeable solid-state flexible sodium metal battery. This work can be extended to the tailoring of FeS_2/C fibers to obtain a better cathode with enhanced electrochemical properties.

Declaration of Competing Interest

The authors declare that they have no known competing financial interests or personal relationships that could have appeared to influence the work reported in this paper.

Acknowledgements

This research was supported by the Basic Science Research Program through the National Research Foundation of Korea (NRF), funded by the Ministry of Education (2017M1A2A2087577, NRF-2017R1A4A1015711 and 2018R1A4A1024691). J. Mohanta, H.-J. Kim,these authors contributed equally to the work.

Appendix A. Supplementary data

Supplementary data to this article can be found online at https://doi.org/10.1016/j.cej.2019.123510.

References

[1] Luo, P. Han, L. Shi, J. Huang, J. Yu, J. Huang, J. Yu, Y. Lin, J. Du, B. Yang, C. Li, C. Zhu, J. Xu, Biomass-derived nitrogen/oxygen co-doped hierarchical porous carbon with a large specific surface area for ultrafast and long-life sodium-ion batteries, Appl. Surf. Sci. 462 (2018) 713–719.
[2] X. Gao, G. Zhu, X. Zhang, T. Hu, Porous carbon materials derived from in situ construction of metal-organic frameworks for high-performance sodium ions batteries, Micropor. Mesopor. Mater. 273 (2019) 156–162.
[3] J. Zhang, W. Wang, B. Li, Effect of particle size on the sodium storage performance of Sn_4P_3, J. Alloy Compd. 771 (2019) 204–208.
[4] H. Wu, L. Zheng, W. Liu, X. Xia, C. Xiao, J. Xie, L. Su, L. Wang, N. Du, Three-dimensional porous copper framework supported group IVA element materials as sodium-ion battery anode materials, J. Alloy Compd. 771 (2019) 169–175.
[5] Z. Dai, U. Mani, H.T. Tan, Q. Yan, Advanced cathode materials for sodium-ion batteries: what determines our choices? Small Methods 1 (2017) 1700098.
[6] Y. Wang, X. Wang, X. Li, R. Yu, M. Chen, K. Tang, X. Zhang, The novel P3-type layered $Na_{0.65}Mn_{0.75}Ni_{0.25}O_2$ oxides doped by non-metallic elements for high performance sodium-ion batteries, Chem. Eng. J. 360 (2019) 139–147.
[7] S.H. Yang, S.-K. Park, Y.C. Kang, Mesoporous $CoSe_2$ nanoclusters threaded with nitrogen-doped carbon nanotubes for high-performance sodium-ion battery anodes, Chem. Eng. J. 370 (2019) 1008–1018.
[8] Y. Wu, P. Nie, L. Wu, H. Dou, X. Zhang, 2D MXene/SnS_2 composites as high-performance anodes for sodium ion batteries, Chem. Eng. J. 334 (2018) 932–938.
[9] A. Kitajou, J. Yamaguchi, S. Hara, S. Okada, Discharge/charge reaction mechanism of a pyrite-type FeS_2 cathode for sodium secondary batteries, J. Power Sources 247 (2014) 391–395.
[10] K. Xi, D. He, C. Harris, Y. Wang, C. Lai, H. Li, P.R. Coxon, S. Ding, C. Wang, R.V. Kumar, Enhanced sulfur transformation by multifunctional FeS_2/FeS/S composites for high-volumetric capacity cathodes in lithium–sulfur batteries, Adv. Sci. 6 (2019) 1800815.
[11] S.S. Zhang, The redox mechanism of FeS_2 in non-aqueous electrolytes for lithium and sodium batteries, J. Mater. Chem. A 3 (2015) 7689–7694.
[12] X. Liu, H.S. Kim, J.H. Hong, Z. Xu, H. Xiao, I.S. Ahn, K.W. Kim, Electrochemical properties of mechanically alloyed Ni-doped FeS2 cathode materials for lithium-ion batteries, Powder Technol. 256 (2014) 545–552.
[13] H. Pang, W. Sun, L.P. Lv, F. Jin, Y. Wang, MOF-templated nanorice–nanosheet core–satellite iron dichalcogenides by heterogeneous sulfuration for high-performance lithium ion batteries, J. Mater. Chem. A 4 (2016) 19179–19188.
[14] P. Zhao, H. Cui, J. Luan, Z. Guo, Y. Zhou, H. Xue, Porous FeS_2 nanoparticles wrapped by reduced graphene oxide as high-performance lithium-ion battery cathodes, Mater. Lett. 186 (2017) 62–65.
[15] W.J. Yu, C. Liu, L. Zhang, P.X. Hou, F. Li, B. Zhang, H.M. Cheng, Synthesis and electrochemical lithium storage behavior of carbon nanotubes filled with iron sulfide nanoparticles, Adv. Sci. 3 (2016) 1600113.
[16] J. Wang, X. Sun, Understanding and recent development of carbon coating on LiFePO4 cathode materials for lithium-ion batteries, Energy Environ. Sci. 5 (2012) 5163–5185.
[17] L. Noerochim, A.O. Yurwendra, D. Susanti, Effect of carbon coating on the electrochemical performance of $LiFePO_4$/C as cathode materials for aqueous electrolyte lithium-ion battery, Ionics 22 (2016) 341–346.
[18] A.K. Haridas, J.E. Lim, D.H. Lim, J. Kim, K.K. Cho, A. Matic, J.K. Kim, J.H. Ahn, An electrospun core–shell nanofiber web as a high-performance cathode for iron disulfide-based rechargeable lithium batteries, ChemSusChem 11 (2018) 3625–3630.
[19] H.G. Wang, W. Li, D.P. Liu, X.L. Feng, J. Wang, X.Y. Yang, X.B. Zhang, Y. Zhu, Y. Zhang, Flexible electrodes for sodium-ion batteries: recent progress and perspectives, Adv. Mater. 29 (2017) 1703012.
[20] J.K. Kim, Y.J. Lim, H. Kim, G.B. Cho, Y. Kim, A hybrid solid electrolyte for flexible solid-state sodium batteries, Energy Environ. Sci. 8 (2015) 3589–3596.
[21] E.M. Jin, H.J. Lee, H.B. Jun, S.M. Jeong, Electrochemical properties of α-$Co(OH)_2$/graphene nano-flake thin film for use as a hybrid supercapacitor, Korean J. Chem. Eng. 34 (2017) 885–891.
[22] J.E. Lim, J.K. Kim, Optimization of electrolyte and carbon conductor for dilithium terephthalate organic batteries, Korean J. Chem. Eng. 35 (2018) 2464–2467.
[23] G. Yuan, J. Xiang, H. Jin, Y. Jin, L. Wu, Y. Zhang, A. Mentbayeva, Z. Bakenov, Flexible free-standing $Na_4Mn_9O_{18}$/reduced graphene oxide composite film as a cathode for sodium rechargeable hybrid aqueous battery, Electrochim. Acta 259 (2018) 647–654.
[24] P. Nie, L. Shen, G. Pang, Y. Zhu, G. Xu, Y. Qing, H. Dou, X. Zhang, Flexible metal–organic frameworks as superior cathodes for rechargeable sodium-ion batteries, J. Mater. Chem. A 3 (2015) 16590–16597.
[25] H.J. Song, D.S. Kim, J.C. Kim, S.H. Hong, D.W. Kim, An approach to flexible Na-ion batteries with exceptional rate capability and long lifespan using $Na_2FeP_2O_7$ nanoparticles on porous carbon cloth, J. Mater. Chem. A 5 (2017) 5502–5510.
[26] Y. Kobayashi, H. Miyashiro, T. Takeuchi, H. Shigemura, N. Balakrishnan, M. Tabuchi, H. Kageyama, T. Iwahori, All-solid-state lithium secondary battery with ceramic/polymer composite electrolyte, Solid State Ion. 152–153 (2002) 137–142.
[27] Z. Hu, Z. Zhu, F. Cheng, K. Zhang, J. Wang, C. Chen, J. Chen, Pyrite FeS_2 for high-rate and long-life rechargeable sodium batteries, Energy Environ. Sci. 8 (2015) 1309–1316.
[28] T. Atesa, M. Keller, J. Kulisch, T. Adermann, S. Passerini, Development of an all-solid-state lithium battery by slurry-coating procedures using a sulfidic electrolyte, Energy Storage Mater. 17 (2019) 204–210.
[29] Z. Shadike, Y.N. Zhou, F. Ding, L. Sang, K.W. Nam, X.Q. Yang, Z.W. Fu, The new electrochemical reaction mechanism of Na/FeS_2 cell at ambient temperature, J. Power Sources 260 (2014) 72–76.
[30] Z. Wang, H. Xiang, L. Wang, R. Xia, S. Nie, C. Chen, H. Wang, A paper-supported inorganic composite separator for high-safety lithium-ion batteries, J. Membr. Sci. 553 (2018) 10–16.
[31] J. Manuel, R.P. Ramasamy, Cycling performance of sodium ion battery comprised of naphthalene based polyimide/MWCNT composite cathode and highly porous polyvinylidene fluoride separator membrane, ECS Trans. 85 (2018) 45–52.
[32] M. Dai, J. Shen, J. Zhang, G. Li, A novel separator material consisting of Zeolitic Imidazolate Framework-4 (ZIF-4) and its electrochemical performance for lithium-ions battery, J. Power Sources 369 (2017) 27–34.
[33] W. Ma, X. Liu, X. Lei, Z. Yuan, Y. Ding, Micro/nano-structured FeS_2 for high energy efficiency rechargeable Li-FeS_2 battery, Chem. Eng. J. 334 (2018) 725–731.
[34] K.L. Hong, L. Qie, R. Zeng, Z.Q. Yi, W. Zhang, D. Wang, Y.H. Huang, Biomass derived hard carbon used as a high performance anode material for sodium ion batteries, J. Mater. Chem. A 2 (2014) 12733–12738.
[35] S. Wu, W. Wang, M. Li, L. Cao, F. Lyu, M. Yang, Z. Wang, Y. Shi, B. Nan, S. Yu, Z. Sun, Y. Liu, Z. Lu, Highly durable organic electrode for sodium-ion batteries via a stabilized α-C radical intermediate, Nat. Commun. 7 (2016) 13318.
[36] Y. Tian, T. Shi, W.D. Richards, J. Li, J.C. Kim, S.-H. Bo, G. Ceder, Compatibility issues between electrodes and electrolytes in solid-state batteries, Energy Environ. Sci. 10 (2017) 1150–1166.
[37] S. Chen, K. Wen, J. Fan, Y. Bando, D. Golberg, Progress and future prospects of high-voltage and high-safety electrolytes in advanced lithium batteries: from liquid to solid electrolytes, J. Mater. Chem. A 6 (2018) 11631–11663.